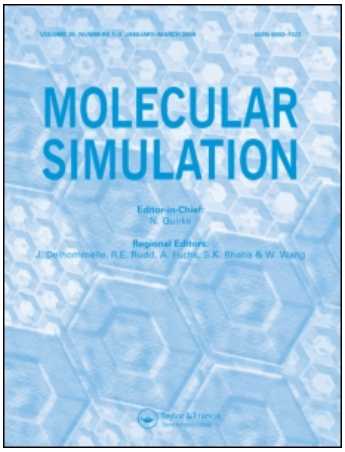

Molecular Simulation
Publication details, including instructions for authors and subscription information:
http://www.informaworld.com/smpp/title~content=t713644482

The Structure of Liquid Methanol: A Molecular Dynamics Study Using Three-Site Models

L. Bianchi[a]; O. N. Kalugin[ab]; A. K. Adya[a]; C. J. Wormald[c]
[a] School of Science and Engineering, Division of Molecular and Life Sciences, University of Abertay Dundee, Dundee, UK [b] Department of Inorganic Chemistry, Kharkov State Univerisity, Kharkov, Ukraine [c] School of Chemistry, University of Bristol, Bristol, UK

To cite this Article Bianchi, L. , Kalugin, O. N. , Adya, A. K. and Wormald, C. J.(2000) 'The Structure of Liquid Methanol: A Molecular Dynamics Study Using Three-Site Models', Molecular Simulation, 25: 5, 321 — 338
To link to this Article: DOI: 10.1080/08927020008024505
URL: http://dx.doi.org/10.1080/08927020008024505

Molecular Simulation, 2000, Vol. 25, pp. 321–338
Reprints available directly from the publisher
Photocopying permitted by license only

THE STRUCTURE OF LIQUID METHANOL: A MOLECULAR DYNAMICS STUDY USING THREE-SITE MODELS

L. BIANCHI[a], O. N. KALUGIN[a,*], A. K. ADYA[a,†] and C. J. WORMALD[b]

[a]*School of Science and Engineering, Division of Molecular and Life Sciences, University of Abertay Dundee, Bell Street, Dundee DD1 1HG, UK;*
[b]*School of Chemistry, University of Bristol, Cantocks Close, Bristol BS8 1TS, UK*

(Received November 1999; accepted November 1999)

The structure of liquid methanol at 298.15 K is investigated by performing molecular dynamics (MD) simulations in NVE ensemble using two 3-site force field models. The simulated structural results are compared with the recent neutron diffraction (ND) results obtained at the partial pair distribution function (pdf) level by employing H/D substitution on the hydroxyl hydrogen, Ho. Overall agreement is found between the simulated and experimental total intermolecular radial distribution functions (rdfs). The ability of the 3-site model simulations to satisfactorily reproduce experimental X—X (X=C, O or H- a methyl hydrogen) intermolecular partial distribution function, dominated by contributions from the methyl group, demonstrates that the methyl group does not participate in any bonding in the liquid. However, a comparison between the simulated and experimental Ho—Ho and X—Ho functions reveals that discrepancies still exist at a quantitative level.

Keywords: Methanol; molecular dynamics; neutron diffraction; computer simulations

INTRODUCTION

Hydrogen bonding is one of the most fundamental interactions in determining the static and dynamic properties of methanol. In order to

*Permanent address: Department of Inorganic Chemistry, Kharkov State University, Kharkov, Svobody Sq., 4, 310077, Ukraine.
†Corresponding author. Tel.: +44-1382-308653, Fax: +44-1382-308663, e-mail: A.Adya@tay.ac.uk

characterise the local order of this solvent, several different geometric models [1, 2] mainly derived by model fitting of X-ray diffraction data [3–5], usually with conflicting results, have been introduced. An attractive alternative for obtaining detailed insight of the structure of the liquid consists in using computer simulations in conjunction with diffraction measurements. Following this idea, Svishchev and Kusalik [6] investigated the orientational correlations in the liquid by constructing spatial distribution functions from the molecular dynamics (MD) simulated O—O and C—O partial distribution functions. They used a potential, devised by Haughney *et al.* [7], which could satisfactorily reproduce the X-ray structural measurements as well as some thermodynamic and dynamic properties of the liquid. This study led to the conclusion that the favored structure in the liquid is an open non-linear zigzag chain of methanol monomers packed spatially in a tetrahedral manner. It has been reported [7] that changes made to the potential induce only small changes in those features that are correlated with hydrogen bond formation. Since such features are hardly detected by X-rays and, contribute too little to be observed in the total neutron radial distribution functions (rdfs), a critical evaluation of different models cannot be done. Thus, reproducing the total intermolecular rdf consisting of 21 partial pair distribution functions (pdf) in methanol is not a proof that a fine tuning of the model potential has been achieved, as was also inferred by Hawlicka *et al.* [8]. A critical test of potential models has to be done at the partial distribution function level. Recently, by using ND isotopic substitution on Ho atom, Adya *et al.* [9] satisfactorily extracted the three intermolecular partial distribution functions: $g_{HoHo}(r)$, $G_{XHo}(r)$ and $G_{XX}(r)$. In this article, we present results of MD simulations carried out on 216 methanol molecules by using the DL_POLY_2.0 MD simulation package [10]. Results obtained by using two different potential models introduced by Haughney *et al.* [7] are compared with those obtained from ND measurements on H/D substituted methanol.

COMPUTATIONAL DETAILS

Each methanol molecule was treated as a rigid, non-polarisable object. Six different MD runs were performed. Two potential models (denoted as J2 and H1) parameterised by Haughney *et al.* [7] were used for the MD simulations. For the first 5 runs, the methanol molecule and the Lennard–Jones (LJ) potential consisted of 3 sites, corresponding to the oxygen (O), the methyl group (C) treated as a united atom and the hydrogen of the hydroxyl group (Ho). For the sixth run ($H1+CH_3$), hydrogens (H) of the methyl group were explicitly taken into account in the geometry of the

molecule (see Fig. 1) and were treated as dead load without any potential interaction. The bond lengths d_{OHo}, d_{CO}, d_{CH} and ∠COHo and ∠HCH (listed in Tab. I) were taken from the millimeter wave studies of Lees and Baker [11]. The calculated moments of inertia along the principal axes, I_A, I_B, I_C, of the methanol molecule, along with their experimental values [11, 12] are also listed in Table I. One can see that the 3-site geometrical model underestimates the moments of inertia because it considers the methyl group

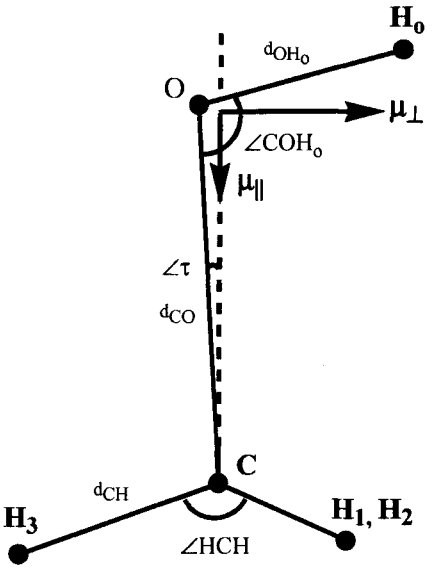

FIGURE 1 The molecular geometry of methanol molecule, from microwave spectra by Lee and Baker [11], used in the MD simulations. H_3, C, O and Ho lie in the symmetry plane of the molecule whereas H_1 and H_2 point in and out of the symmetry plane.

TABLE I Molecular geometry and dipole moment of the methanol molecule

Model parameter	*Experimental*[a]	*Experimental*[b]	*J2*[c] (3 *sites*)	*H1*[c] (3 *sites*)	*H1* + CH_3 (6 *sites*)
d_{OHo}, Å	0.937	0.9451 ± 0.0034	0.9451	0.9451	0.9451
D_{CO}, Å	1.434	1.4246 ± 0.0024	1.4246	1.4246	1.4246
D_{CH}, Å	–	1.0936 ± 0.0032	1.0936	1.0936	1.0936
∠COHo, °	105.93	108.53 ± 0.48	108.53	108.53	108.53
∠HCH, °	109.5	108.63 ± 0.70	–	–	108.63
∠τ, °	–	3.27 ± 0.18	–	–	3.27
I_A, amu · Å^2	3.961	3.96277	0.7368	0.7368	3.9178
I_B, amu · Å^2	20.533	20.4834	16.7356	16.7356	20.4780
I_C, amu · Å^2	21.283	21.2679	17.4725	17.4725	21.2147
$\mu_\parallel$, D	−0.885	–	–	–	–
$\mu_\perp$, D	1.44	–	–	–	–
μ, D[a]	1.69	–	2.22	2.33	2.33
∠$\vec{\mu}$, $O\vec{H}_o$	50.6	–	50.9	55.8	55.8

[a]Ref. [12]; [b]Ref. [11]; [c]Ref. [7].

as a united carbon atom. For the 6-site geometrical model, however, good agreement with experimental values is found.

Runs 1 and 2 were performed with J2 whereas all others were performed with H1. For all the runs, the used partial Coulombic charges coincided with the LJ sites so that the intermolecular potential was given by a sum of LJ and Coulombic terms

$$V_{ij}(r_{ij}) = \frac{q_i q_j}{4\pi\varepsilon_0 r_{ij}} + 4\varepsilon_{ij}[(\sigma_{ij}/r_{ij})^{12} - (\sigma_{ij}/r_{ij})^6], \quad (1)$$

where ε_{ij} and σ_{ij} are the Lennard–Jones (LJ) parameters between sites i and j of distinct molecules, q_i is the partial charge on site i and, r_{ij} is the site–site separation. Table II summarises the force field parameters used in the MD simulations. Cross interactions were obtained from the Lorentz–Berthelot [13] rules $\varepsilon_{ij} = \sqrt{\varepsilon_{ii}\varepsilon_{jj}}$ and $\sigma_{ij} = (\sigma_{ii} + \sigma_{jj})/2$.

The electrostatic interactions in the J2 and H1 models being similar, they give similar values for the dipole moments of 2.2 D and 2.3 D, respectively. These values are larger than the gas phase experimental value of 1.69 D (see Tab. I). This enhancement in the dipole moment was intentionally made [7] to take approximate account of induction forces in methanol. A shifted force (SF) potential was employed for run 1 to avoid truncation errors [13]. A reaction field (RF) model [14] was applied to runs 2–4 and, Ewald summation (EW) was used for runs 5 and 6. The MD simulations were performed at 298.15 K in the NVE ensemble with 216 methanol molecules placed in a cubic box of edge length 24.45 Å in order to match experimental density [15], 0.78637 g/cm^3. A cut-off radius equal to half the box length was applied to all the interactions and, periodic boundary conditions were applied. In all the MD runs, the time step used was 0.002 ps. The details of the MD algorithms employed for the various runs are given in Table III.

TABLE II Force field parameters for the methanol molecule

Parameter	*J2*	*H1*	*H1* + CH_3
σ_{HoHo}, Å	0.0	0.0	0.0
σ_{OO}, Å	3.071	3.083	3.083
σ_{CC}, Å	3.775	3.861	3.861
σ_{HH}, Å	–	–	0.0
ε_{HoHo}, kJ/mol	0.0	0.0	0.0
ε_{OO}, kJ/mol	0.71130	0.73117	0.73117
ε_{CC}, kJ/mol	0.86611	0.75786	0.75786
ε_{HH}, kJ/mol	–	–	0.0
q_{Ho}(e)	+0.435	+0.431	+0.431
q_O(e)	−0.700	−0.728	−0.728
q_C(e)	+0.265	+0.297	+0.297
q_H(e)	–	–	0.0

TABLE III Details of the MD runs for liquid methanol at 298.15 K. Values of simulated configurational (potential) energy, pressure and diffusion coefficient are compared with the experimental data

	Run 1	*Run* 2	*Run* 3	*Run* 4	*Run* 5	*Run* 6	*Experiment*
Force-field model	J2	J2	H1	H1	H1	H1 + CH_3 (6 sites)	–
Long-range (Coulomb) interactions treatment	SF	RF	RF	RF	EW	EW	–
Algorithm	Vlf + SHAKE	Vlf + SHAKE	Vlf + SHAKE	FIQA, rigid body	Vlf + SHAKE	FIQA, rigid body	–
Equilibration time, ps	94	110	100	150	60	70	–
Sampling time, ps	40	50	100	50	100	40	–
$\langle T \rangle$, K	287.5 ± 8.7	289.5 ± 8.8	295.8 ± 8.7	298.8 ± 9.6	292.7 ± 9.0	301.1 ± 9.2	–
$-\langle U \rangle$, kJ/mol	35.9 ± 0.2	36.4 ± 0.2	35.3 ± 0.3	35.1 ± 0.2	35.5 ± 0.2	35.3 ± 0.2	34.95[a]
$\langle P \rangle$, kbar	0.14 ± 0.37	0.19 ± 0.38	0.74 ± 0.39	0.77 ± 0.39	0.77 ± 0.36	0.85 ± 0.39	–
$D \times 10^9$, m^2/s[b]	1.31 (1.04)	1.38 (1.29)	1.13 (0.91)	1.15 (1.08)	1.24 (1.30)	2.01 (1.92)	2.42 ± 0.05[c]

[a] Experimental potential energy was calculated from the experimental enthalpy of vaporization (ΔH_{vap}), ΔH_{vap} was taken from [15]; [b]First values were obtained from the center of mass (c.o.m) velocity auto-correlation function (VACF), values in brackets were obtained using the c.o.m mean square displacement (MSD); [c]from [16]; Vlf stand for Verlet leap-frog algorithm [17]; SHAKE for the algorithm used to constrain the methanol geometry [18]; EW for Ewald summation; SF for shifted force potential; RF for reaction field model; FIQA stands for Fincham's Implicit Quaternion algorithm [19].

VALIDATION OF THE SIMULATED RESULTS

The computed configurational energy, U, shows good agreement (see Tab. III) with its experimental counterpart [15] evaluated from the enthalpy of vaporisation, $\Delta_{vap}H^{exp}$ by $U_{exp} = \Delta_{vap}H^{exp} - PV = \Delta_{vap}H^{exp} - RT$. This relation is based on the assumption that intramolecular energy is the same in both the liquid and the gas phase, and that the gas obeys the ideal gas law. The translational diffusion coefficient of the center-of-mass of the methanol molecules was calculated from the mean square displacement (MSD) *via* the Einstein relation [13] and also according to the Green–Kubo relation [13]

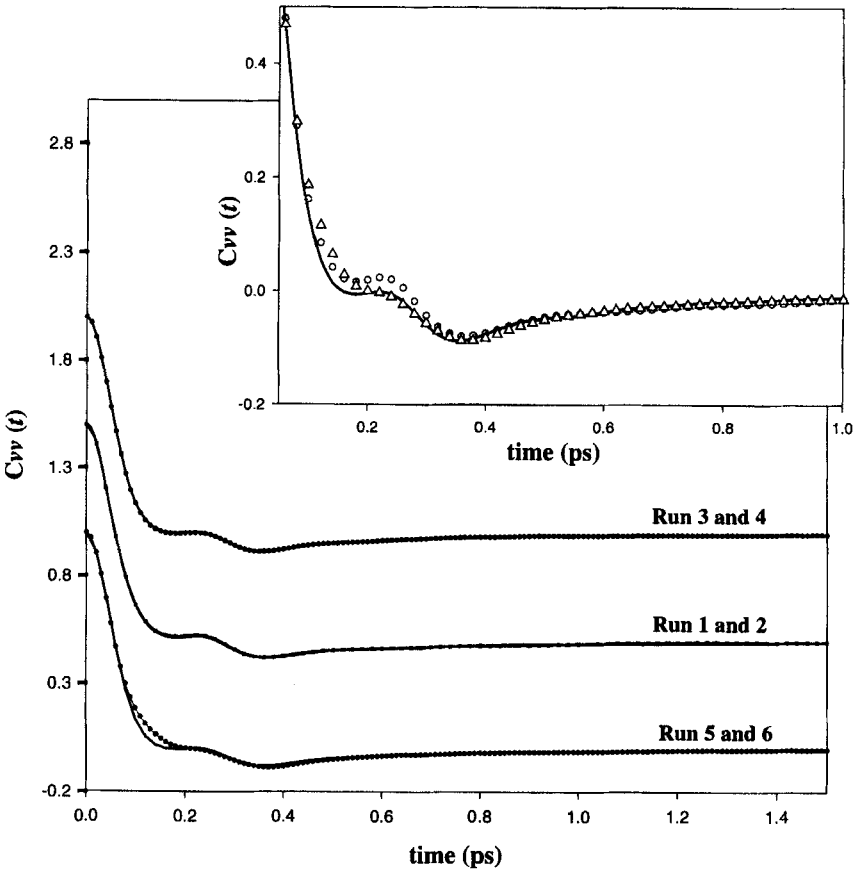

FIGURE 2 Normalised center-of-mass (c.o.m) velocity auto correlation functions $C_{vv}(t)$, obtained for the six MD runs (bottom: runs 5 (-) and 6 (•); middle: runs 1 (■) and 2 (-) displaced by 0.5; top: runs 3 (-) and 4 (•) displaced by 1). Inset shows runs 1 (○), 4 (-) and 6 (Δ) superimposed on an enlarged scale.

by integrating the velocity autocorrelation function (VACF), $\hat{C}_{vv}(t)$. The normalised VACF, $C_{vv}(t)$ defined as,

$$C_{vv}(t) = \langle \mathbf{v}(t)\mathbf{v}(0)\rangle / \langle \mathbf{v}(0)\mathbf{v}(0)\rangle = \hat{C}_{vv}(t)/\langle \mathbf{v}(0)^2\rangle \quad (2)$$

and the MSD are shown in Figures 2 and 3, respectively. The calculated diffusion coefficients are listed in Table III together with experimental data. One can see that runs 1–5 fail to reproduce the diffusion coefficient. This effect is clearly seen in the smaller slopes in the MSD curves of runs 1–5 as compared to that of run 6 (see Fig. 3). This can be attributed to the fact that the calculated moments of inertia in runs 1–5 are not in agreement with the experimental values [11, 12]. Also, the main difference in the VACFs (see Fig. 2) lies in a feature at 0.24 ps which is a clearly defined peak in runs 1–5, but becomes a shoulder in run 6. All the runs however, in agreement with previous dynamical studies [7, 20–22], show the typical cage effect (observed after 0.2 ps) coming from a close packing of the molecules. In general, the diffusion coefficients estimated from the MSD are in reasonable agreement with those determined from the VACF. Agreement

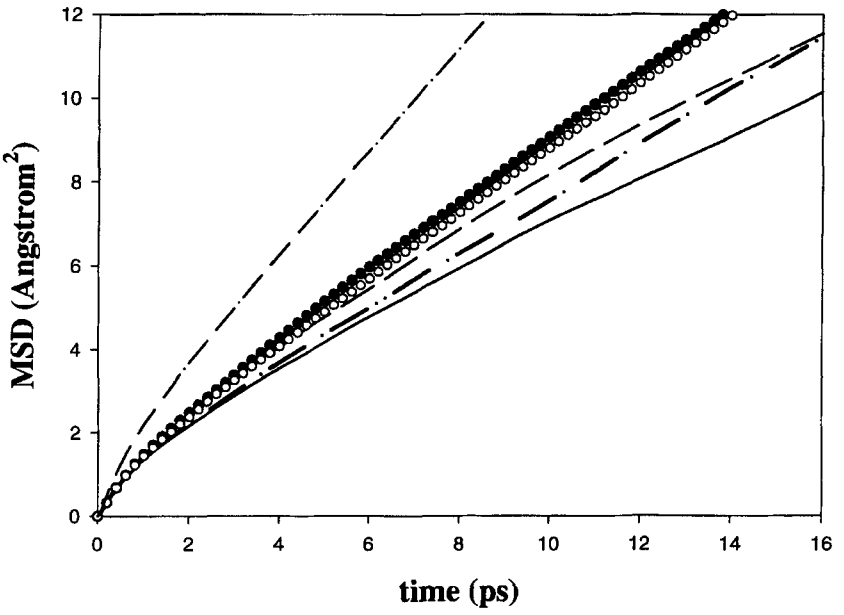

FIGURE 3 Center-of-mass (c.o.m) mean square displacements (MSD) obtained for the six MD runs (run 1: solid line, run 2: •, run 3: dashed line, run 4: dash-dot-dot, run 5: o and run 6: dash and dots).

between the calculated diffusion coefficients for run 6 using both methods of calculation and experiment [16] is also satisfactory (see Tab. III).

The pdfs, $g_{\alpha\beta}(r)$ were computed for all the runs from the equilibrated configurations. It may be recalled that since in run 6, the 3 methyl hydrogens are treated as dead load, it yields 21 pdfs while all other runs yield 6 pdfs. In addition, since run 6 also reproduced both thermodynamic and dynamic properties rather well, most of the discussion in the next section will be focused on the pdfs (shown in Figs. 4 and 8(b)) obtained from this run. However, it will be instructive to compare results from other runs, where possible.

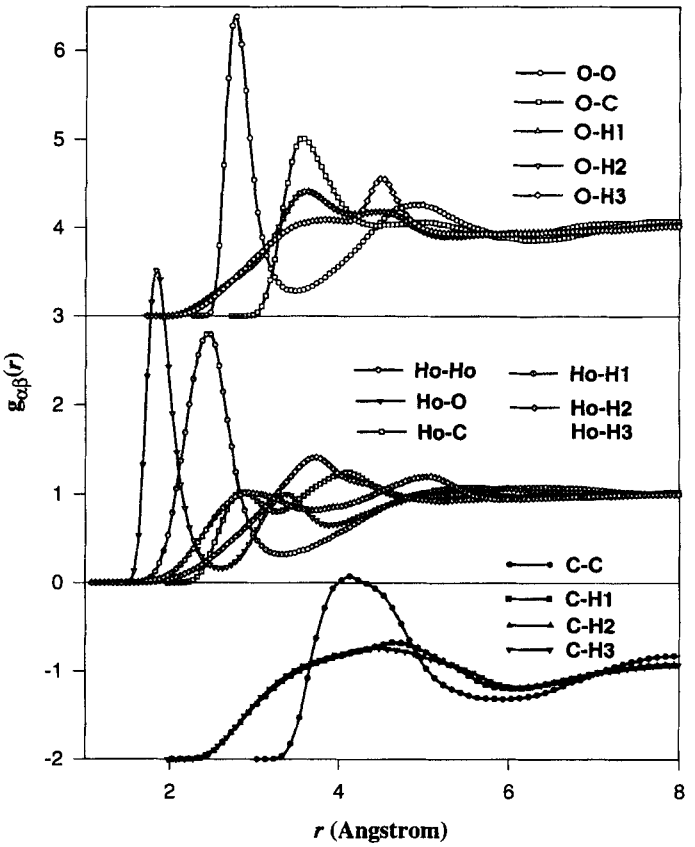

FIGURE 4 The simulated intermolecular partial pair distribution functions, $g_{\alpha\beta}(r)$ obtained from run 6: the O-other atom pdfs in the top box displaced by +3; the Ho-other atom pdfs in the middle box, and C-other atom pdfs in the bottom box displaced by −2. The H—H pdfs are included in Figure 8(b).

RESULTS AND DISCUSSION

The results of current simulations are compared with earlier X-ray diffraction [3–5, 23, 24] and MD simulation [6, 22, 25–30] studies in Tables IV and V. Although the results differ at a quantitative level, the agreement seems to be satisfactory. For instance, while the run 6 simulation shows the main peak position of O—C pdf at 3.6 Å, the X-ray studies [24] report it at 3.8 Å. The height, co-ordination number and position of the simulated O—C pdf are in reasonable agreement with other computer simulations

TABLE IV Characteristics of the C—C and C—O partial pdfs in liquid methanol obtained with H1 + CH_3 model for the MD run 6 as compared to available experimental data and computer simulation studies

Pdf	$r_{M1}(exp.)/Å$	$r_{M1}/Å$	$g(r_{M1})$	$n(r)$	$n(r)^h$
C—O	3.8[a]	3.6[h]	2.01[h]		
		3.62[b]	1.94[b]	6.1(4.5)[b]	5.22(4.53)
		3.62[g]	–	5.1(4.5)[g]	5.22(4.53)
		3.64[c]	–	4.0(4.2)[c]	4.1(4.23)
		3.6[d]	–	–	–
C—C	3.8, 4.4[a,f]	4.18[h]	2.07[h]		
		4.10[g]	–	12.0(5.88)	12.3(5.88)
		4.15[b]	–	12.8(6.0)[b]	12.7(5.99)
		4.1[d]	–	–	–
		4.1[e]	–	–	–

[a]Ref. [24]; [b]Ref. [22]; [c]Ref. [25]; [d]Ref. [26]; [e]Ref. [27]; [f]broad peak consisting of one peak at 3.8 Å and another at 4.4 Å; [g]Ref. [28]; [h]this work (run 6); r_{M1} is the position of 1st maximum; $g(r_{M1})$, the height of first maximum and; $n(r)$, the co-ordination number calculated up to r in Å (value in brackets).

TABLE V Characteristics of the O—O partial pdf in liquid methanol obtained with H1 + CH_3 model for the MD run 6 as compared to available experimental data and other computer simulation studies

$r_{M1}(exp.)/Å$	$n(r)(exp.)$	$r_{M1}/Å$	$r_{M2}/Å$	$g(r_{M1})$	$n(r)$	$n(r)^l$
2.76–2.80[a]	–	2.79[l]	4.87[l]	3.38[l]		
		2.7[d]	4.9[d]	–	2.0(3.4–3.5)	2.0(3.43)
2.66[b] (cryst)	–	2.8[e]	–	–	–	–
		2.88[m]	4.78	–	1.9(3.46)	2.0(3.43)
		2.75[f]	4.7[f]	–	2.0[f]	2.05
		2.85[g]	4.9[g]	3.25[g]	2.0(3.41)[g]	2.0(3.43)
		2.75[h]	4.7[h]	–	2.0(3.4)[h]	2.0(3.43)
		2.81[i]	–	–	–	–
2.798[c]	1.8(3.25[k])					1.87(3.23)

[a] Ref. [4]; [b]Ref. [31]; [c]Ref. [5]; [d]Ref. [27]; [e]Ref. [6]; [f]Ref. [29]; [g]Ref. [22]; [h]Ref. [30]; [i]Ref. [26]; [j]at the minimum of the first peak; [k]distance assumed; [l]this work (run 6); [m]Ref. [28]; r_{Mi} is the position of ith maximum; $g(r_{M1})$ = height of first maximum and; $n(r)$, the co-ordination number calculated up to r in Å (value in brackets).

(Tab. IV). The simulated O—O pdf shows a main peak at 2.79 Å with a coordination number of 1.87, which again agrees with the X-ray work of Narten *et al.* [5] (see Tab. V). The simulated C—C pair exhibits a broad peak at 4.18 Å (see Fig. 4). It has been suggested [24] that two distinct C—C contributions occur at ~3.8 Å and ~4.4 Å which may lead to such broadening. The simulated results for the C—C pair (see Tab. IV) are again consistent with experimental and other computer simulation studies. It is not surprising that the earlier simulations reproduced the X-ray structure rather well since firstly, no other structural measurements capable of discriminating between different models were available at that time and secondly, the models were parameterised to obtain a better agreement with the liquid structure obtained from X-ray studies. Only two MD studies [7, 8] compared the simulated structures with ND measurements [32, 33] only at the total rdf level. It needs to be stressed that such a comparison at the total rdf level cannot provide useful information. In the following, we compare the simulated structure with the new ND results, both, at the total and the partial distribution function level.

Total Radial Distribution Functions (rdfs)

ND measurements performed on CD_3OD, CD_3OH and $CD_3O(H/D)$, discussed in detail elsewhere [9], yielded the total rdfs containing both intra and inter molecular contributions. The intramolecular contribution for each sample was removed [9] by using exactly the same geometrical model for the methanol molecule, as is used in the current MD simulations. The three rdfs can be written as:

$$^{i}G^{\text{inter}}(r) = \sum_{\alpha,\beta} {}^{i}W_{\alpha\beta}\, g_{\alpha\beta}(r) \tag{3}$$

where the superscript i refers to the sample i. For CD_3OD, CD_3OH and $CD_3O(H/D)$, $i = 1, 2, 3$, respectively. The simulated pdfs, $g_{\alpha\beta}(r)$ from run 6 were combined in the ratio of their neutron weights, ${}^{i}W_{\alpha\beta}$ (listed in Ref. [9]) in order to reconstruct the total intermolecular rdfs for the three samples. The three MD distribution functions plotted in Figure 5 show a good agreement with their neutron counterparts. It can be seen that even the negative peak for CD_3OH at ~1.7 Å seen in the ND results is predicted by the MD simulation. The oscillations, occurring at larger distances are also mimicked in phase with the ND results, although these are somewhat damped. However, since the total rdfs consist of several different contributions, a comparison at the total rdf level can reveal nothing further.

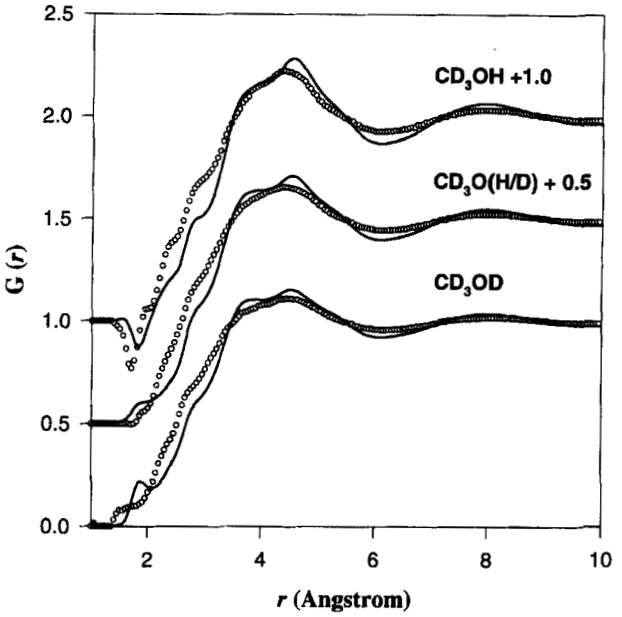

FIGURE 5 The total intermolecular radial distribution functions for CD_3OD, CD_3OH, $CD_3O(H/D)$ obtained from MD run 6 (lines) and ND experiments (circles).

Partial Distribution Functions

The H/D substitution on hydroxyl hydrogen (Ho) has been used [9] to extract the three partial distribution functions, $g_{HoHo}(r)$, $G_{XHo}(r)$ and $G_{XX}(r)$. The simulated pdfs were combined in the ratio of their neutron weights to construct their MD equivalents. These results are discussed below.

Ho—Ho Partial

The simulated Ho—Ho pdfs obtained from all the 6 runs are compared with the neutron results in Figure 6. All six MD runs show impressive agreement with each other although it is worth noting that runs 1 – 5 failed to reproduce the experimental translational diffusion coefficient. No structural differences can be seen between the results obtained by using J2 and H1 models. Moreover, various algorithms and techniques applied within the same force field (runs 1 – 2 for J2 or 3 – 6 for H1, in Tab. III), do not produce any change in the Ho—Ho pdf. Since methanol is considered to be a strongly associated liquid due to its polarity, we expected that the

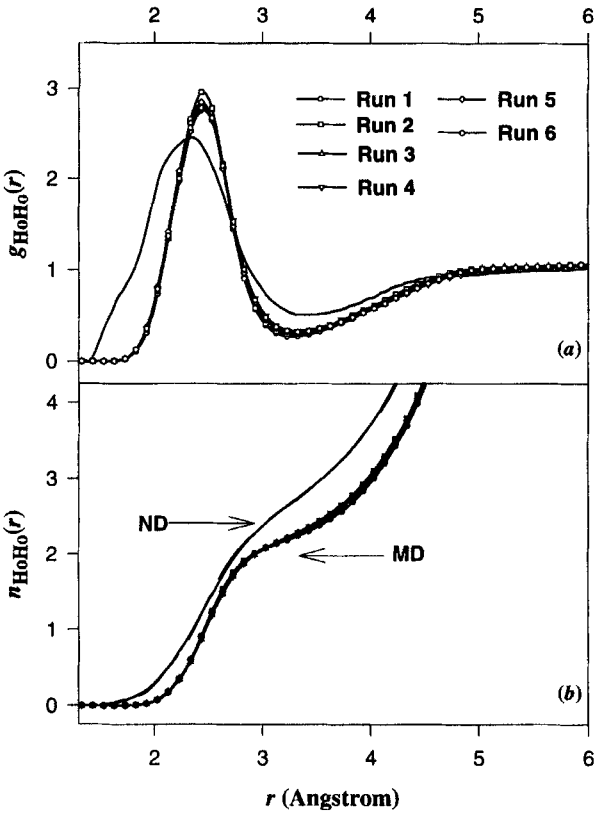

FIGURE 6 (a) Ho—Ho partial pair distribution function obtained from the six MD runs (lines and points) as compared to the one obtained from ND H/D-substitution experiments (line). (b) The running co-ordination number of Ho—Ho pair, n_{HoHo}, obtained from the ND data (solid line) and the six MD runs (line and points).

Ho—Ho pdf obtained by using different techniques to handle long-range interactions would at least differ. However, we do not see any significant difference in the size, shape or peak positions in the Ho—Ho pdfs. Although MD and ND results are fairly in agreement (Fig. 6(a)) with each other, discrepancies still exist at a quantitative level. For instance, (i) the main peak maxima are shifted ~ 0.13 Å toward high r, (ii) the MD peaks are bigger and more symmetric, (iii) the height at the first minimum is lower and, (iv) there are fewer correlations at shorter distances in MD simulations as compared to the neutron results. This comparison reveals that the MD simulation does not allow closer approach of the two hydroxyl hydrogens and, suggests less mobility between the first and next-nearest neighbours.

The running co-ordination numbers, n_{HoHo} for ND and MD Ho—Ho pdf, displayed in Figure 6(b), confirm these findings. Table VI compares the peak position and co-ordination number obtained from current simulations of run 6 with other simulations and experimental studies. It can be seen that the co-ordination numbers obtained from our MD simulation compare well with those obtained from others. Nevertheless, all the simulations underestimate this value in comparison to ND results. Also, there are discrepancies between the peak positions of the Ho—Ho pdf obtained not only from various simulations but also with the experiment.

X—Ho Partial

The $G^{inter}_{XHo}(r)$ (X = C, H and O) distribution function obtained from simulated partials for run 6, added in the ratio of their neutron weights, is compared in Figure 7 with its neutron equivalent function [9]. Comparison of ND with MD results in the low r-range (up to ~2.5 Å), which is dominated by the O—Ho contribution (see Fig. 4), shows that the agreement is only qualitative. The MD O—Ho peak is much higher and shifted to high r in comparison to the experimental peak. These differences can also be seen in Figure 7 inset, where the intra + intermolecular rdf from ND and MD are compared. The peak at ~1.9 Å is clearly overemphasized in MD as compared to the experimental one and, the shoulder at 1.7 Å is also not reproduced. Figure 7 also shows that MD run 6 reproduces qualitatively the shape of the experimental curve beyond ~2.8 Å. For instance, although the MD reproduces the shape of the first peak at ~3.5 Å along with the shoulder on its right, the peak is higher and shifted slightly to high r. It is also seen that the MD run 6 simulation mimics (see Fig. 7),

TABLE VI Characteristics of the Ho—Ho pdf in liquid methanol obtained with the H1 + CH_3 model for the MD run 6 as compared to available experimental data and other computer simulation studies

$r_{M1}(exp.)/Å$	$g(r_{M1})(exp.)$	$r_{M1}/Å$	$g(r_{M1})$	$n(r)$	$n(r)^h$	$n^{ND}(r)^c$
		2.49[h]	2.79[h]			
2.4[a]	–	2.45[d]		–	–	–
		2.45[e]		2.3(3.31)[e]	2.26(3.28)	2.74(3.31)
2.36[c]	2.46	2.35–2.40[f]		2.1–2.2(3.25)[f]	2.26(3.28)	2.69(3.28)
		2.50[b]		2.3(3.38)[b]	2.32(3.38)	2.8(3.38)
		2.26[g]		2.4(2.89)[g]	1.94(2.88)	2.2(2.88)

[a] Ref. [33]; [b]Ref. [28]; [c]Ref. [9]; [d]Ref. [29]; [e]Ref. [22]; [f]Ref. [30]; [g]Ref. [26]; [h]this work (run 6); r_{M1} is the position of 1st maximum; $g(r_{M1})$ = height of first maximum and; $n(r)$, the coordination number calculated up to r in Å (value in brackets).

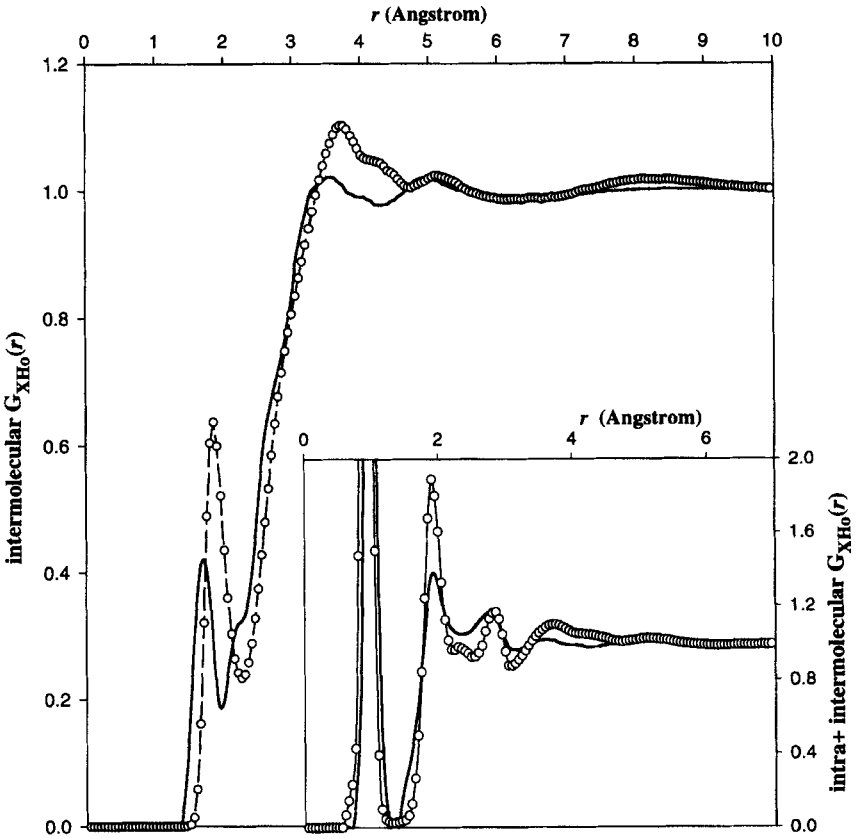

FIGURE 7 Intermolecular X—Ho partial distribution function obtained from MD run 6 (circles) and ND experiments (solid line). The intra- + intermolecular X—Ho function is compared in the inset, circles: from run 6 MD and lines: from the use of ND H/D-substitution experiments.

rather well, the peak at ~ 5 Å, the shape of the experimental curve and the dropping tail at the low r-end.

X—X Partial

The non-substituted atom–non-substituted atom (X—X) distribution function is a weighted sum of six pdfs, $g_{X1\,X2}(r)$:

$$G_{XX}^{\text{inter}}(r) = \sum_{X_1 \neq Ho} \sum_{X_2 \neq Ho} W_{X_1X_2}\, g_{X_1X_2}(r), \quad \text{where } X_1, X_2 = C, O, H. \qquad (4)$$

The $G_{XX}(r)$ constructed from the MD simulation of run 6 is compared with the ND results in Figure 8(a) and, reasonable overall agreement is found. Since H—H, C—H, and H—O correlations contribute $\sim 85\%$ to the X—X partial, the $G_{XX}(r)$ is dominated by contributions from the methyl group. A look at the pdfs (Figs. 4 and 8(b)) reveals that the contribution to $G_{XX}(r)$ below ~ 2 Å arises mainly from the H—H correlations. It would thus appear that in the $H1 + CH_3$ model, the absence of any hard core potential on the methyl hydrogens leads to a closer approach of these atoms

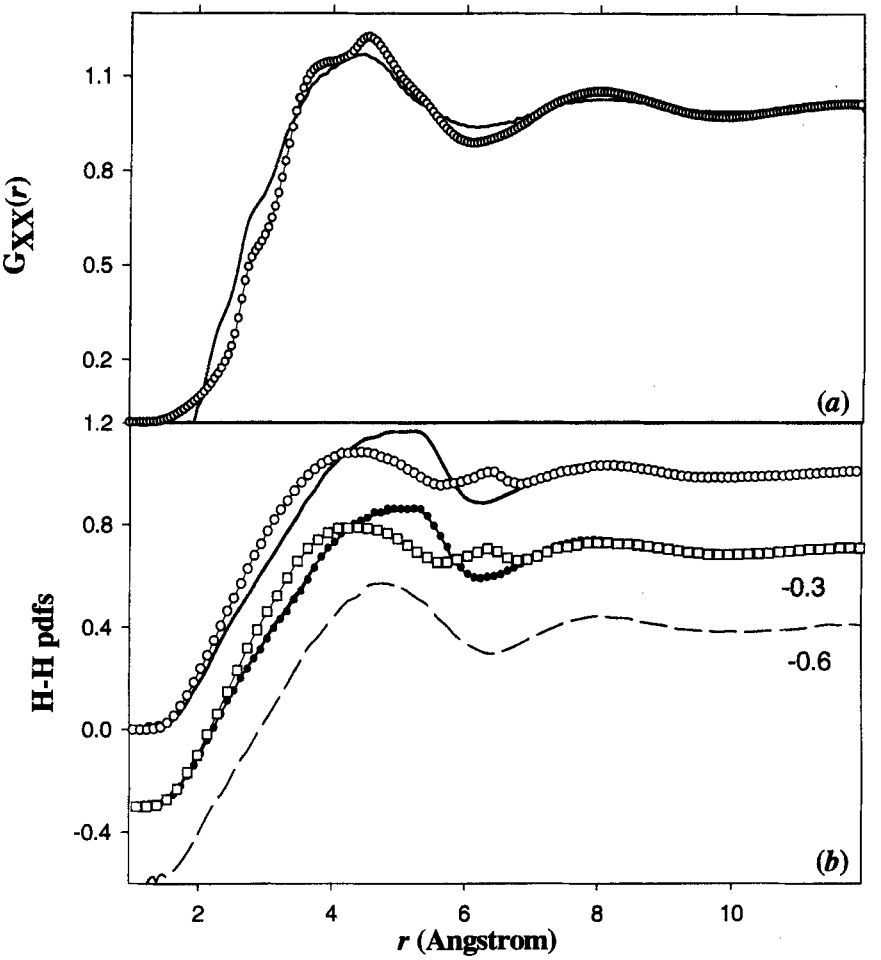

FIGURE 8 (a) X—X partial distribution function obtained from MD run 6 (solid line) as compared to the one obtained from ND experiments (circles). (b) The H—H pdfs obtained from MD run 6 (bottom: H_3—H_3; middle: H_1—H_1 (circles), H_1—H_2 (solid line), H_1—H_3 (squares); top: H_2—H_2 (solid line), H_2—H_3 (circles)).

relative to that observed experimentally (see Fig. 8(a)). Figure 8(a) also reveals that the amplitude of MD oscillations is slightly larger than the ND ones, suggesting that the simulated liquid is more structured. However, both the simulated and experimental partials have the same period of oscillation as that observed already in the total intermolecular rdfs shown in Figure 5. This proves firstly, that the total rdf is dominated predominantly by the methyl group contributions. Secondly, since no potential is imposed on the methyl hydrogens in the $Hl + CH_3$ model, the agreement between the simulated and experimental partials demonstrates, as suggested before [3, 34], that the methyl groups do not participate in any intermolecular bonding.

CONCLUSIONS

Two different 3-site potential models were used to perform six different molecular dynamics simulation runs that differed in the techniques employed for integrating the equations of motion and for treatment of the long range interactions. While the first five of them considered the methyl group to be a united carbon atom, the sixth treating the methyl hydrogens explicitly as dead load reproduced the diffusion coefficient and the total intermolecular radial distribution functions obtained from neutron diffraction (ND) experiments. A comparison of the simulated $G_{XX}(r)$, $G_{XHo}(r)$ and $g_{HoHo}(r)$ partials (where Ho is the hydroxyl hydrogen and X, any other atom) with the corresponding ND results shows that the methyl hydrogens do not participate in any intermolecular bonding. The carbon atom treated as a united interaction site is found to be a good approximation for predicting the correlation involving all atoms other than the hydroxyl hydrogen. The simulated liquid is more structured and discrepancies between MD and ND exist at a quantitative level in all the partial distribution functions. It is evident that although the models considered in this work give a qualitative picture of the structure of liquid methanol, these models, which have been used widely in the past, are inappropriate and warranty further refinement to achieve quantitative agreement with experimental results.

Acknowledgments

We are grateful to the EPSRC for continued support of our structural work on a variety of liquids. One of us, LB is grateful to the University of Abertay-Dundee for the Ph.D. studentship, and, ONK acknowledges the Royal Society/NATO for the award of a post-doctoral fellowship.

References

[1] Sarkar, S. and Joarder, R. N. (1993). "Molecular clusters and correlations in liquid methanol at room temperature", *J. Chem. Phys.*, **99**, 2032.

[2] Tanaka, Y., Ohtomo, N. and Arakawa, K. (1985). "The structure of liquid alcohols by neutron and X-ray diffraction. III. Liquid structure of methanol", *Bull. Chem. Soc. Japan*, **58**, 270.

[3] Zachariasen, W. H. (1935). "The liquid "structure" of methyl alcohol", *J. Chem. Phys.*, **1**, 158.

[4] Magini, M., Paschina, G. and Paccaluga, G. (1982). "On the structure of methyl alcohol at room temperature", *J. Chem. Phys.*, **77**, 2051.

[5] Narten, A. H. and Habenschuss, A. (1984). "Hydrogen bonding in liquid methanol and ethanol determined by X-ray diffraction", *J. Chem. Phys.*, **80**, 3387.

[6] Svishchev, I. M. and Kusalik, P. G. (1994). "Structure in liquid methanol from spatial distribution functions", *J. Chem. Phys.*, **100**, 5165.

[7] Haughney, M., Ferrario, M. and Mc Donald, I. R. (1987). "Molecular dynamics simulation of liquid methanol", *J. Phys. Chem.*, **91**, 4934.

[8] Hawlicka, E., Palinkas, G. and Heinzinger, K. (1989). "A molecular dynamics study of liquid methanol with a flexible six-site model", *Chem. Phys. Lett.*, **144**, 255.

[9] Adya, A. K., Bianchi, L. and Wormald, C. J. (2000). "Structure of liquid methanol by H/D substitution technique of neutron diffraction" *J. Chem. Phys.* (in Press).

[10] Smith, W. and Forester, T. R. (1996). "DL_POLY_2.0: a general purpose parallel molecular dynamics simulation package", *J. Mol. Graphics*, **14**, 137.

[11] Lees, R. M. and Baker, J. G. (1968). "Torsion-vibration-rotation interactions in methanol I. Millimeter wave spectrum", *J. Chem. Phys.*, **48**, 5299.

[12] Ivash, E. V. and Dennison, D. M. (1953). "The methyl alcohol molecule and its microwave spectrum", *J. Chem. Phys.*, **21**, 1804.

[13] Allen, M. P. and Tildesley, D. J., "*Computer simulation of liquids*", Oxford University Press, 1987.

[14] Neumann, M. (1985). "The dielectric constant of water, computer simulation with the MCY potential", *J. Chem. Phys.*, **82**, 5663.

[15] Riddick, J. A., Bunger, W. B. and Sakano, T. K., "*Organic solvents, physical properties and methods of purification*", 4th edition, Wiley: New York, 1986.

[16] Hurle, R. L. and Woolf, L. A. (1980). "The effect of isotopic substitution on self-diffusion in methanol under pressure", *Aust. J. Chem.*, **33**, 1947.

[17] Hockney, R. W. (1970). "The potential calculation and some applications", *Methods Comput. Phys.*, **9**, 136.

[18] Ryckaert, J. P., Ciccotti, G. and Berendsen, H. J. C. (1977). "Numerical integration of the Cartesian equations of motion of a system with constraints: molecular dynamics of *n*-alkanes", *J. Comput. Phys.*, **23**, 237.

[19] Fincham, D. (1981). "An algorithm for rotational motion of rigid molecules", *CCP5 Quartely*, **2**, 6.

[20] Palinkas, G., Baco, I. and Heinzinger, K. (1991). "Molecular dynamics investigation of the inter-intramolecular motions in liquid methanol and methanol-water mixtures", *Mol. Phys.*, **73**, 897.

[21] Alonso, J., Bermejo, F. J., Garcia-Hernandez, M., Martinez, J. L. and Howells, W. S. (1991). "H-bond in methanol: a molecular dynamics study", *J. Molec. Struc.*, **218**, 147.

[22] Palinkas, G., Hawlicka, E. and Heinzinger, K. (1987). "A molecular dynamics study of liquid methanol with a flexible three-site model", *J. Phys. Chem.*, **91**, 4334.

[23] Harvey, G. C. (1938). "Fourier analysis of liquid methyl alcohol", *J. Chem. Phys.*, **6**, 111.

[24] Wertz, D. L. and Kruh, R. K. (1967). "Reinvestigation of structures of ethanol and methanol at room temperature", *J. Chem. Phys.*, **47**, 388.

[25] Jorgensen, W. L. (1980). "Structure and properties of liquid methanol", *J. Am. Chem. Soc.*, **102**, 543.

[26] Jorgensen, W. L. (1981). "Transferable intermolecular potential functions. Application to liquid methanol including internal rotation", *J. Am. Chem. Soc.*, **103**, 341.

[27] Gao, J., Habibollazadeh, D. and Shao, L. (1995). "A polarizable intermolecular potential function for simulation of liquid alcohols", *J. Phys. Chem.*, **99**, 10400.

[28] Shilov, I. Y., Rode, B. M. and Durov, V. A. (1999). "Long range order and hydrogen bonding in liquid methanol: a Monte-Carlo simulation", *Chem. Phys.*, **241**, 75.
[29] Marchi, M. and Klein, M. (1989). "A computer simulation study of supercooled liquid and amorphous solid methanol", *Z. Naturforsh.*, **44(a)**, 585.
[30] Jorgensen, W. L. (1986). "Optimized intermolecular potential functions for liquid alcohols", *J. Phys. Chem.*, **90**, 1273.
[31] Tauer, K. J. and Lipscomb, W. (1952). "On the crystal structures, residual entropy and dielectric anomaly of methanol", *Acta Crystall.*, **5**, 606.
[32] Montague, D. G., Gibson, I. P. and Dore, J. C. (1981). "Structural studies of liquid alcohols by neutron diffraction. I. Deuterated methyl alcohol CD_3OD", *Mol. Phys.*, **44**, 1355.
[33] Montague, D. G., Dore, J. C. and Cummings, S. (1984). "Structural studies of liquid alcohols by neutron diffraction. III. CD_3OH, CD_3OD and $CD_3O(H/D)$ mixtures", *Mol. Phys.*, **53**, 1049.
[34] Steytler, D. C., Dore, J. C. and Montague, D. G. (1985). "Neutron diffraction studies of amorphous methyl alcohol", *J. Non-Cryst. Solids*, **74**, 303.